Supporting information

"Light on" fluorescence carbon dots with intramolecular hydrogen bond-regulated co-planarization for cell imaging and temperature sensing

Chan Wang[a], Yimin He[a], Yalan Xu[a], Laizhi Sui[b], Tao Jiang[a], Guoxia Ran[a] and Qijun Song*[a]

a Key Laboratory of Synthetic and Biological Colloids, Ministry of Education, International Joint Research Center for Photoresponsive Molecules and Materials, School of Chemical & Material Engineering, Jiangnan University, Wuxi, 214122, PR China

b State key Laboratory of Molecular Reaction Dynamics, Dalian Institute of Chemical Physics, Chinese Academy of Sciences, Dalian, 116023, PR China

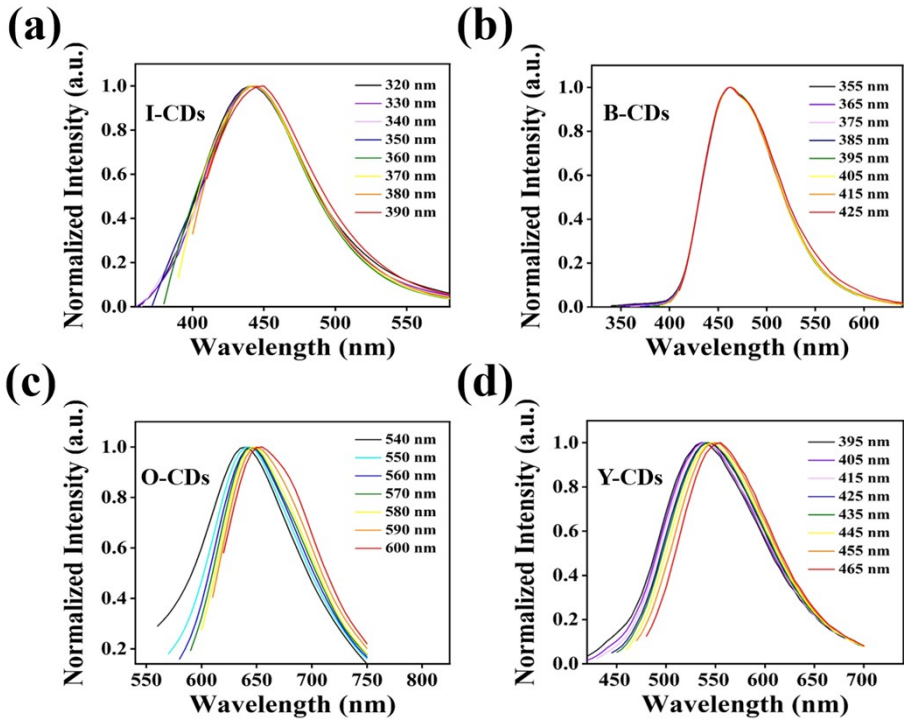

Figure S1 Normalized PL emission spectra of different CDs at different excitation wavelengths.

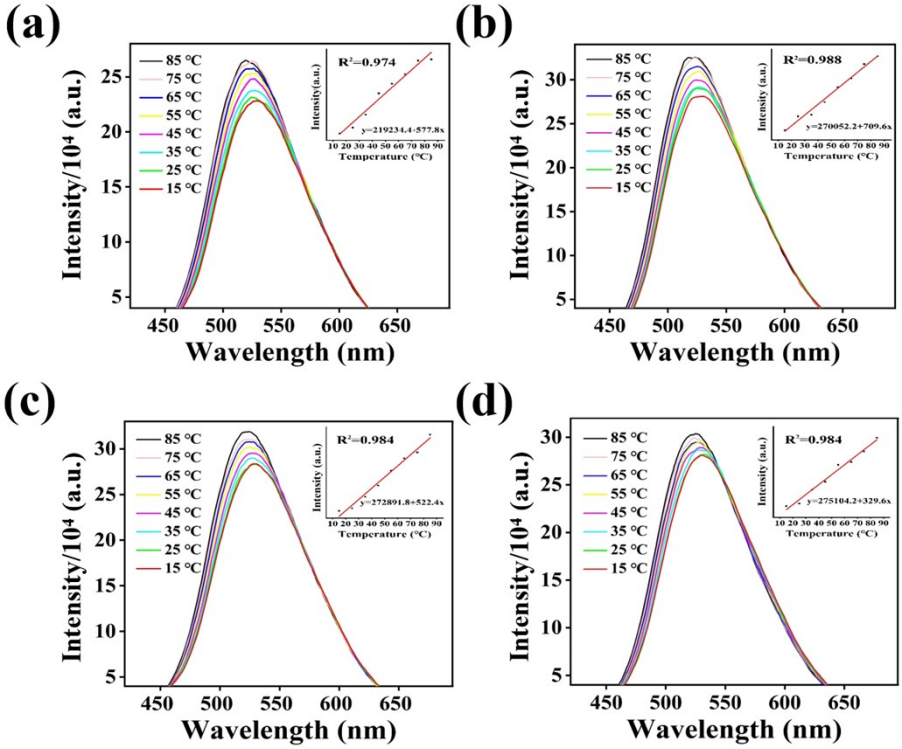

Figure S2 The effect of the molar ratio of CA/Urea on the fluorescence intensity of Y-CDs during the heating processes. (a) 0.1, (b) 0.14, (c) 0.2 and (d) 0.4.

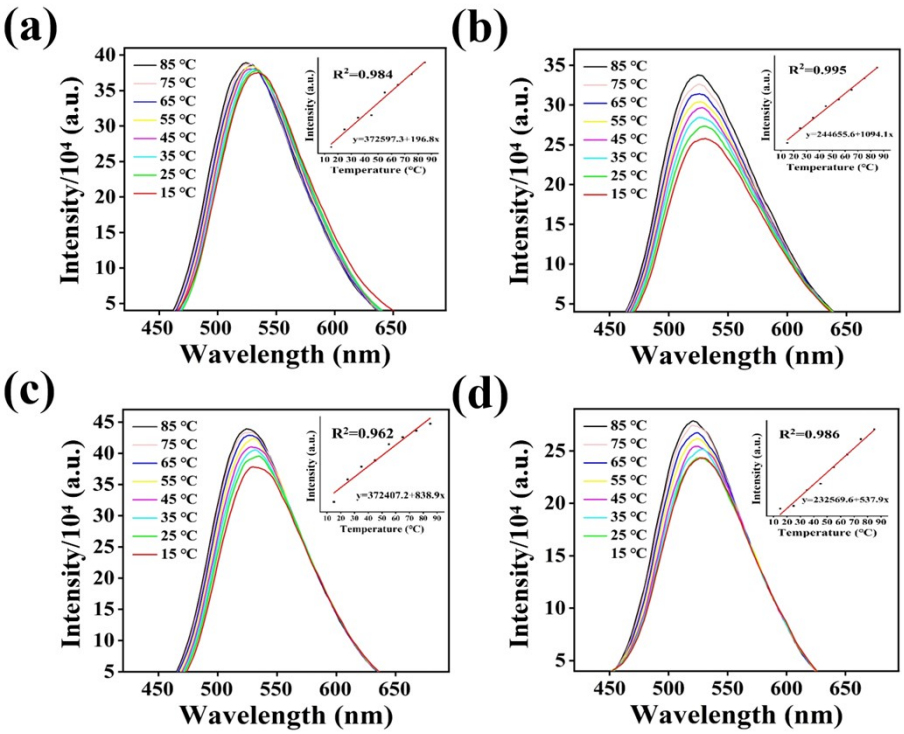

Figure S3 The effect of reaction temperature on the fluorescence intensity of Y-CDs during the heating processes. (a) 150 °C, (b) 160 °C, (c) 170 °C and (d) 180 °C.

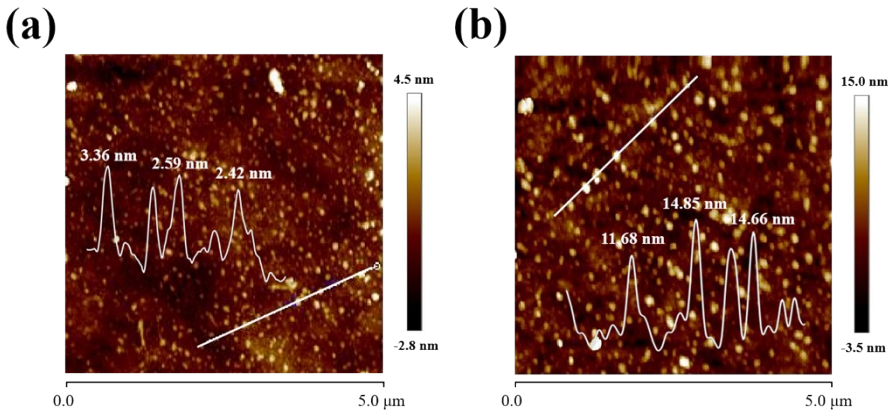

Figure S4 AFM images of (a) B-CDs and (b) Y-CDs, inset: the height profile along the line.

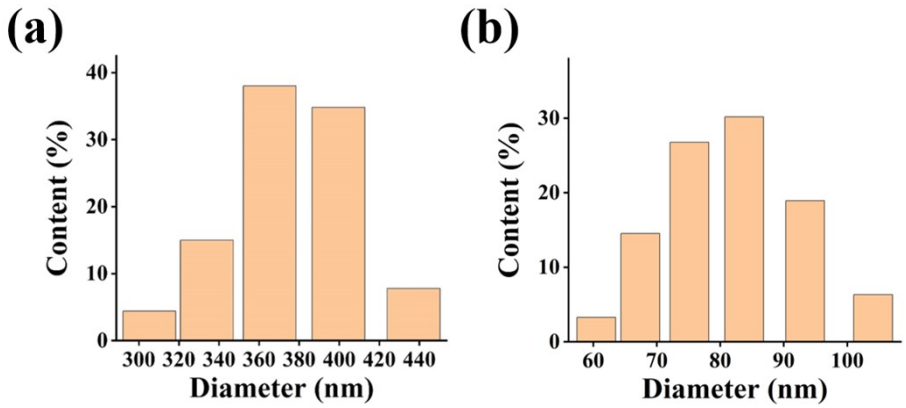

Figure S5 Hydrated radius of Y-CDs (a) and B-CDs (b) measured from DLS analyzer.

Table S1 The atomic percentages of B-CDs and Y-CDs.

Sample	C	N	O
Y-CDs	68.27%	8.03%	23.7%
B-CDs	84.05%	3.22%	12.73%

Table S2 XPS data analyses of the C 1s spectra of B-CDs and Y-CDs.

Sample	C-C/C=C	C-N/C-O	C=O	COOH
Y-CDs	0.378	0.071	0.301	0.250
B-CDs	0.606	0.070	0.232	0.092

Table S3 Fitted parameters of the fluorescence decay curves of Y-CDs at different temperatures.

T(℃)	f_1(%)	τ_1 (ns)	f_2(%)	τ_2 (ns)	τ_{ave} (ns)
20	6.25	4.6366	93.75	8.3583	8.12
40	10.12	5.1493	89.88	8.5011	8.16
60	6.42	4.5467	93.58	8.3737	8.13

Table S4 Fitted parameters of the fluorescence decay curves of B-CDs at different temperatures.

T(℃)	f_1(%)	τ_1 (ns)	f_2(%)	τ_2 (ns)	τ_{ave} (ns)
20	32.08	0.5074	67.92	4.8395	3.45
40	34.65	0.4988	65.35	4.3557	3.02
60	40.02	0.4858	59.98	3.7272	2.43

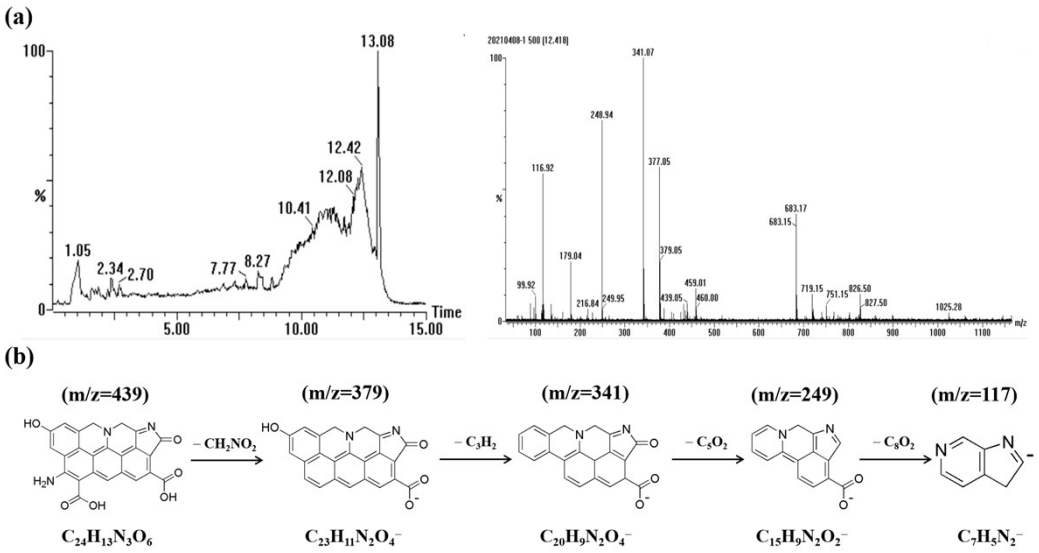

Figure S6 (a) LC-MS spectra of Y-CDs at different retainment time (left) and the spectra corresponding to $T^{12.42}$ (right). (b) The presumable decomposition process of Y-CDs.

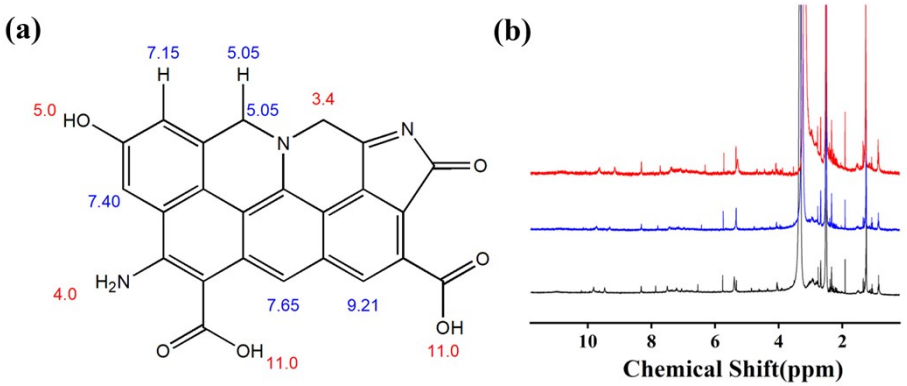

Figure S7 (a) The chemical shifts of different hydrogen atoms in Y-CDs estimated by ChemDraw Ultra 7.0, and the estimation quality can be denoted by the color of value (blue=good, red=rough). (b) ^{1}H-NMR spectra of Y-CDs in DMSO-d_6 at different temperatures (black line: 298k, blue line: 313k, red line: 328k).

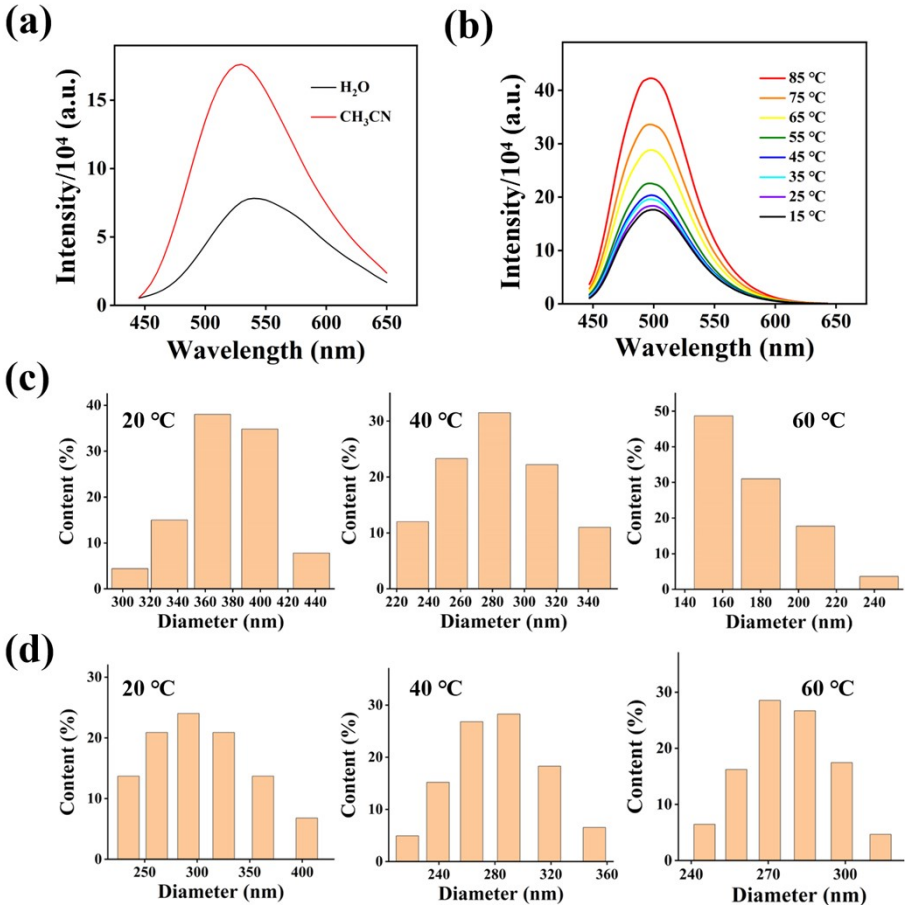

Figure S8 (a) Fluorescence spectra of Y-CDs in H_2O and CH_3CN. (b) Fluorescence spectra of Y-CDs in CH_3CN at different temperatures. Hydrated radius of Y-CDs in aqueous solution (c) and CH_3CN (d) at different test temperatures from DLS measurements.

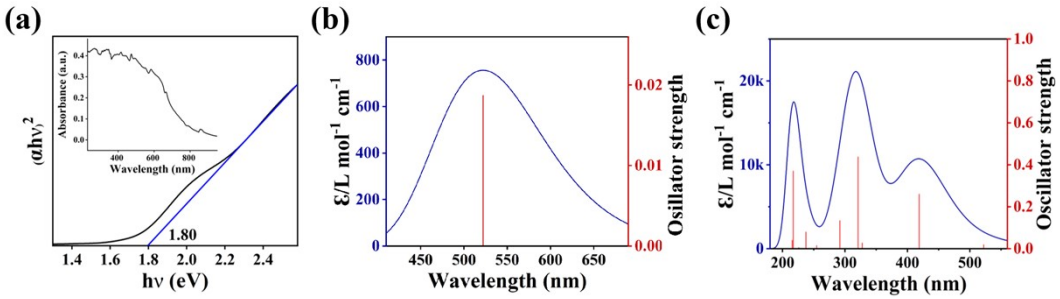

Figure S9 (a) Plot of $(\alpha h\nu)^{1/2}$ versus (hν) for the band gap energy. Inset: UV–Vis DRS. (b) The calculated fluorescence spectrum of Y-CDs. (c) The calculated absorption spectrum of Y-CDs.

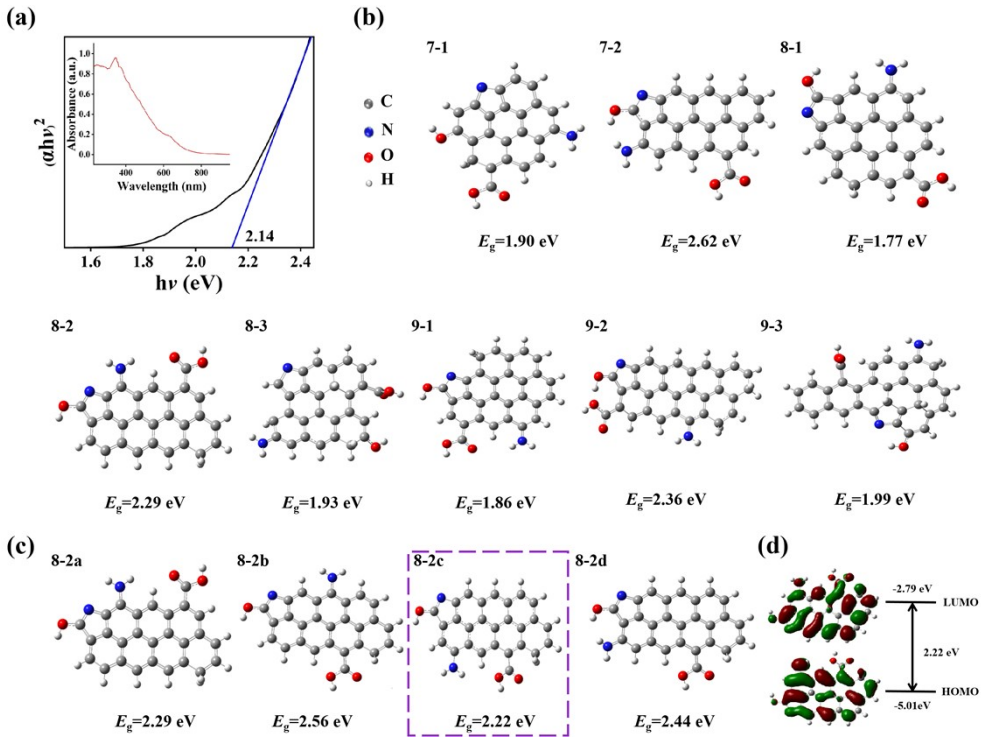

Figure S10 (a) Plot of $(\alpha h\nu)^{1/2}$ versus $(h\nu)$ for the band gap energy. Inset: UV–Vis DRS. (b)The optimized models of B-CDs ranging from seven to nine polyaromatic rings based on DFT calculations. (c) Optimized eight-ring structures with substituents locating at different sites. (d)The calculated HOMO and LUMO energy levels for optimized 8-2c.

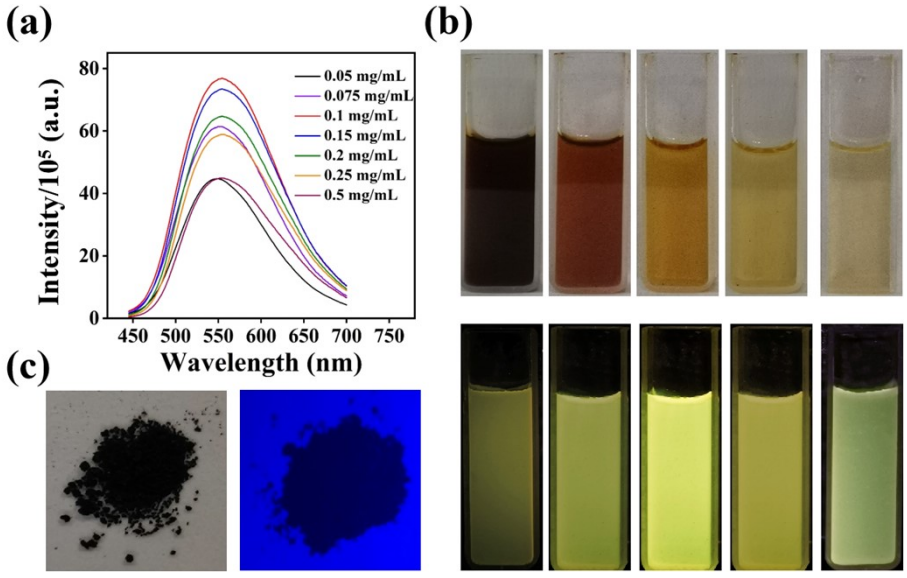

Figure S11 (a) Fluorescence spectra of Y-CDs solution at different concentrations. (b) The concentration-dependent properties of Y-CDs. The concentrations from left to right are 5, 1, 0.5, 0.1, 0.05 and 0.01 mg/mL, respectively. (c) Photos of Y-CDs powders under daylight (left) and UV light (right).

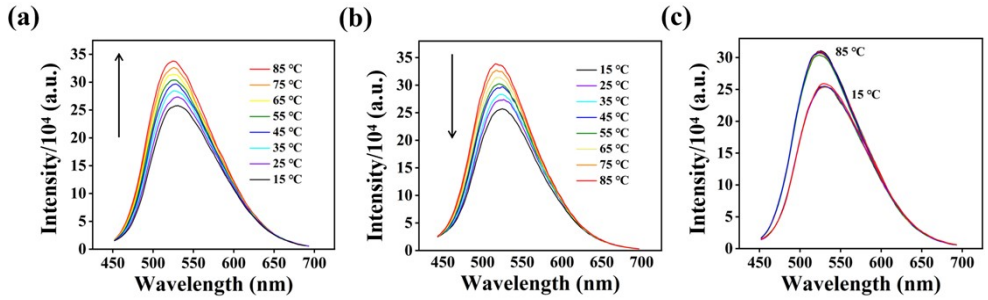

Figure S12 Fluorescence spectra of Y-CDs solution during heating (a) and cooling (b) processes. (c) Fluorescence spectra of Y-CDs solution at 15 °C and 85 °C during six cycles.

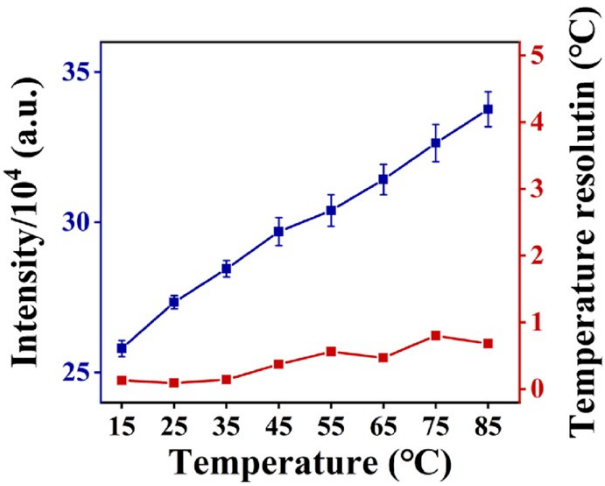

Figure S13 The temperature resolution of Y-CDs in the range from 15 °C to 85 °C.

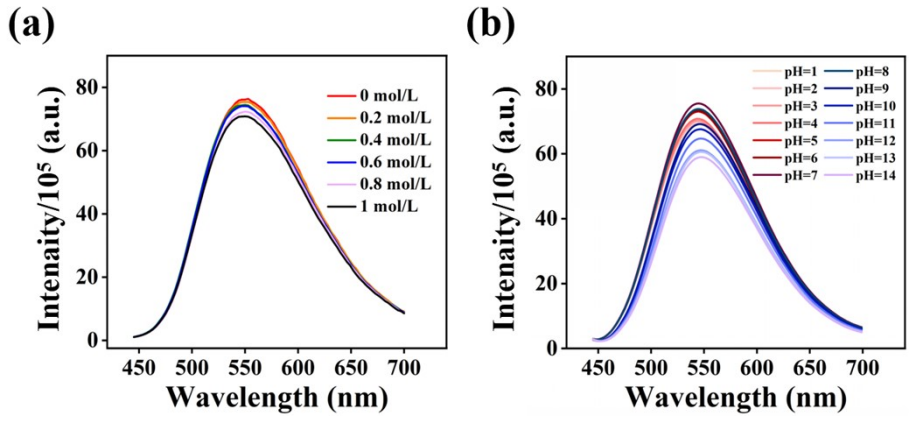

Figure S14 Fluorescence spectra of Y-CDs solution at different NaCl concentrations (a) and pH values (b).

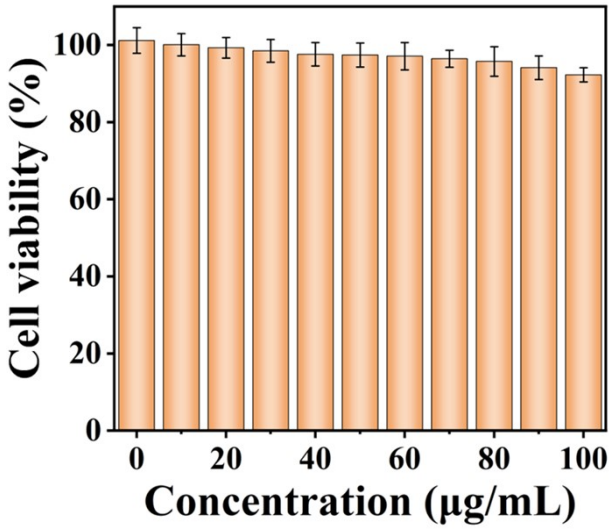

Figure S15 Viability of HeLa cells after 24 h incubation at different concentrations of the Y-CDs.

Table S5 The thermosensitivity of as-prepared "light-on" fluorescence CDs with different carbon sources.

Thermosensitive signal	Code name	Precursors	Synthesis method	Eluent (CH_2Cl_2 :CH_3OH)	$\lambda_{ex}/\lambda_{em}$ (nm)	Thermal sensitivity (%/℃)	Linear responses	Intramolecular hydrogen bonds
Turn-on	Y-CDs	Urea/CA	Solvothermal 160 ℃, 6 h	1:1	425/540	0.45	y=0.11x+24.4 R^2=0.994	√
	CDs-2	1,2-diaminobenzene /hydroquinone	Solvothermal 180 ℃, 6 h	8:1	450/557	0.81	y=0.37x+39.36 R^2=0.989	√
	CDs-3	1,2-diaminobenzene /CA	Solvothermal 180 ℃, 6 h	8:1	450/547	1.1	y=0.14x+9.41 R^2=0.987	√
	CDs-4	2,4-diaminotoluene /CA	Solvothermal 160 ℃, 5 h	5:1	480/580	0.89	y=0.31x+27.40 R^2=0.992	√
	CDs-5	2,4-diaminotoluene /benzoic acid	Solvothermal 160 ℃, 5 h	5:1	445/507	3.0	y=0.14x+1.85 R^2=0.989	√
	CDs-6	2,4-diaminotoluene /phloroglucinol	Solvothermal 160 ℃, 5 h	5:1	500/580	1.5	y=0.23x+11.48 R^2=0.999	√
	CDs-7	4-aminobenzoic acid/resorcinol	Solvothermal 160 ℃, 5 h	3:1	375/475	1.1	y=0.23x+17.35 R^2=0.991	√
	CDs-8	CA/resorcinol	Solvothermal 160 ℃, 6 h	6:1	425/550	5.3	y=0.46x−1.99 R^2=0.991	√

Table S6 Comparison of thermosensitivity with different CDs materials.

Temperature-sensitive signal	Carbon precursor	Solvent	λ_{em} (nm)	Temperature range (℃)	Thermal Sensitivity (%/℃)	Ref.
Turn-on	Urea/CA	CH_3CN	500	15–85	2.0	This work
	2,4-Diaminotoluene/ benzoic acid	H_2O	550	15–85	5.3	This work
	CA/thionine	H_2O	650	4–80	1.2	1
	Carbon nanopowders	H_2O	430	25–95	0.75	2
	α-mangostin	/	599	0–150	0.53	3
	Formamide/glutathione	H_2O	460, 685	5–60	3.7	4
Turn-off	Cetylpyridinium/chloride	H_2O	460	20–80	0.33	5
	CA/N-acetyl-L-cysteine	H_2O	420	5–75	0.41	6
	Sodium citrate/L-cysteine /rhodamine B	H_2O	450, 595	10–100	1.4	7
	Glucose/glutathione	H_2O	494	15–90	0.69	8
	Methionine/acrylic acid	H_2O	485	25–75	1.2	9
	CA/urea	H_2O	440, 590	15–85	0.93	10
	Ethanediamine/urea	H_2O	475	20–80	0.85	11
	CA/ N-aminoethylpiperazine	H_2O	440	25–95	0.23	12
	D. officinale	H_2O	448, 660	5–75	0.57	13
	CA/ethylenediamine	/	445	0–80	0.68	14
	Ethylenediamine	H_2O	400, 465	5–85	1.5	15
	Sucrose	H_2O	450, 517	8–60	2.1	16

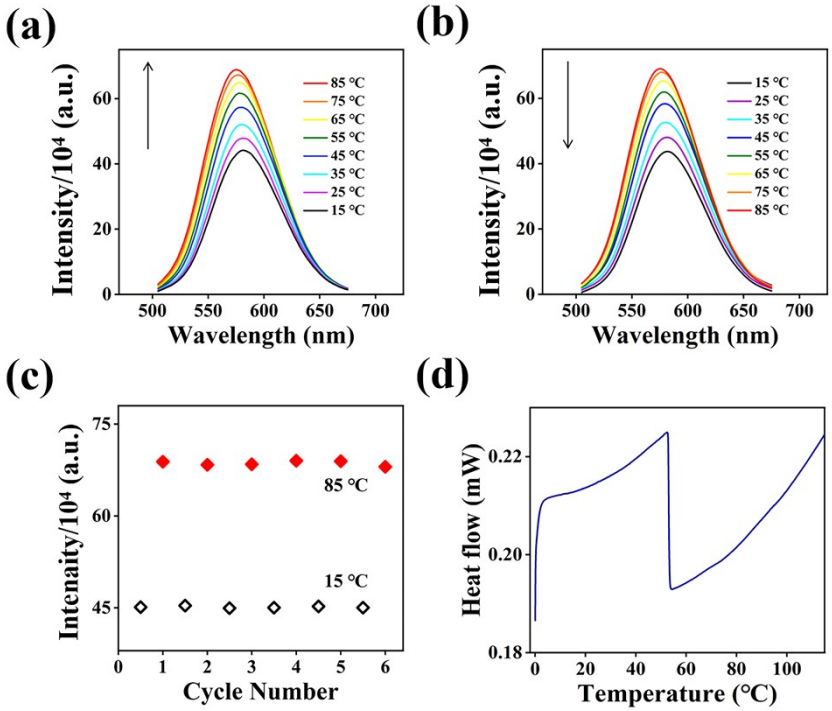

Figure S16 Fluorescence spectra of CDs-2 solution during heating (a) and cooling (b) processes. (c) Fluorescence spectra of CDs-2 solution at 15 °C and 85 °C during six cycles. (d) DSC curve of CDs-2.

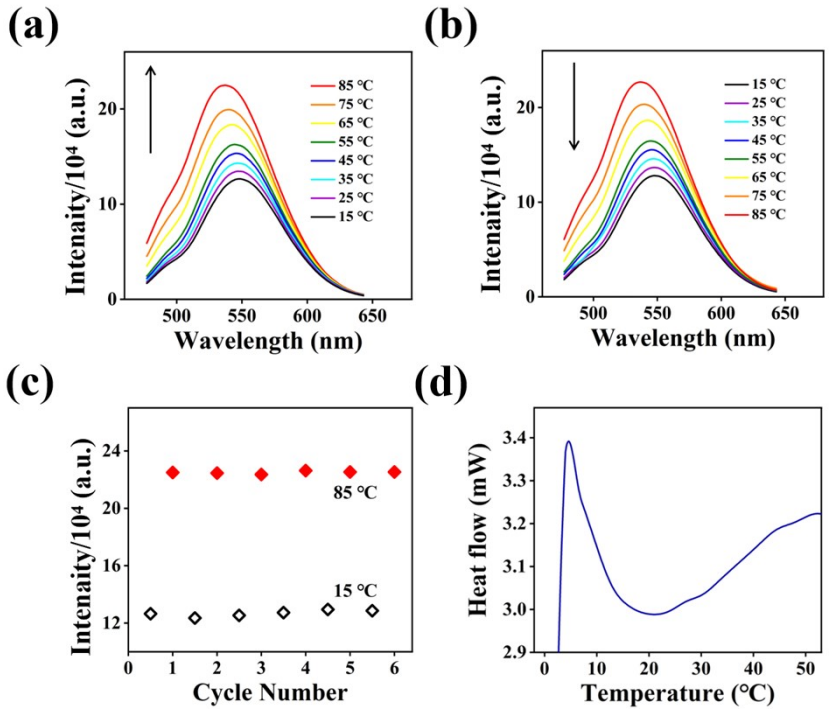

Figure S17 Fluorescence spectra of CDs-3 solution during heating (a) and cooling (b) processes. (c) Fluorescence spectra of CDs-3 solution at 15 °C and 85 °C during six cycles. (d) DSC curve of CDs-3.

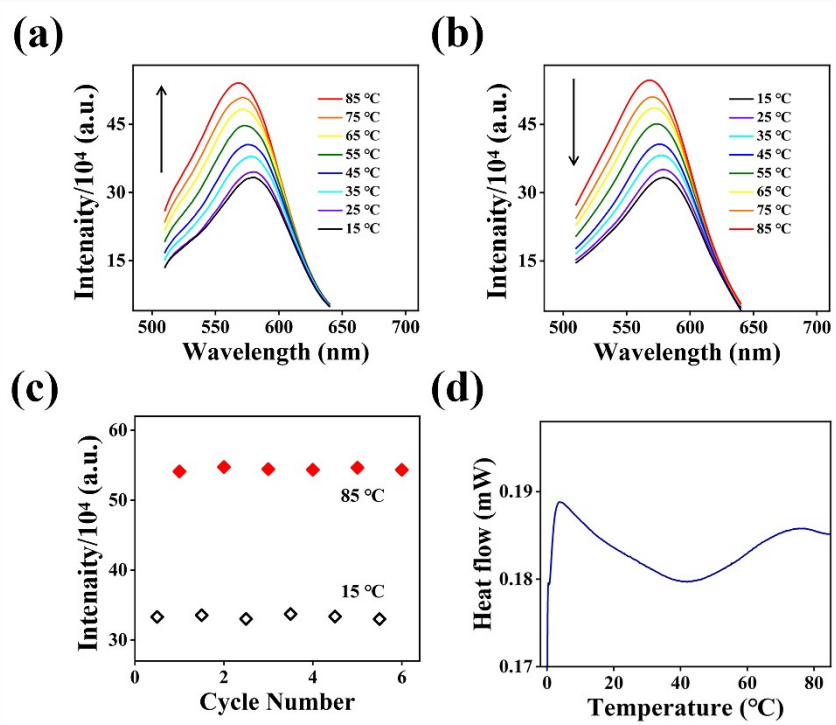

Figure S18 Fluorescence spectra of CDs-4 solution during heating (a) and cooling (b) processes. (c) Fluorescence spectra of CDs-4 solution at 15 °C and 85 °C during six cycles. (d) DSC curve of CDs-4.

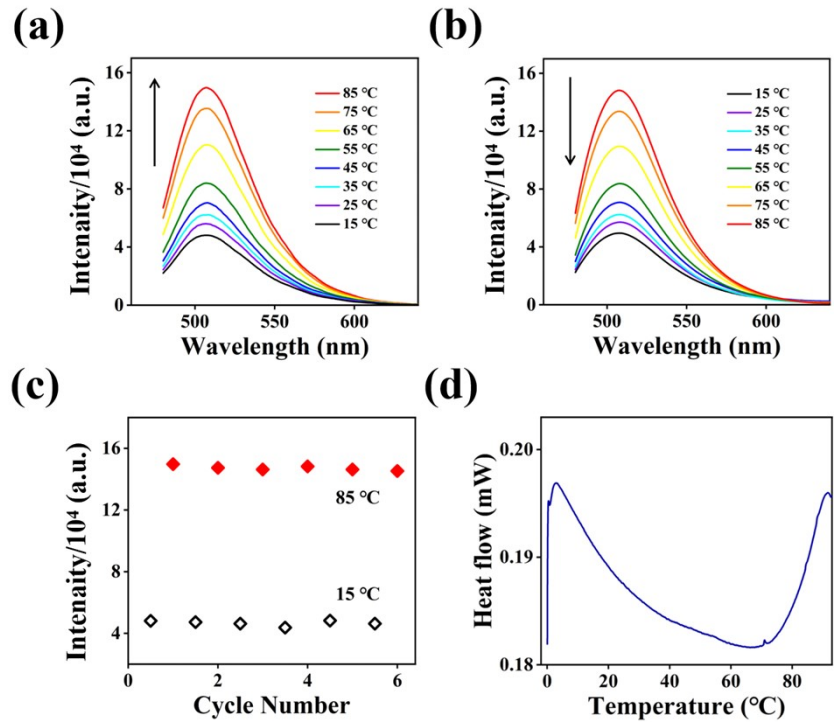

Figure S19 Fluorescence spectra of CDs-5 solution during heating (a) and cooling (b) processes. (c) Fluorescence spectra of CDs-5 solution at 15 °C and 85 °C during six cycles. (d) DSC curve of CDs-5.

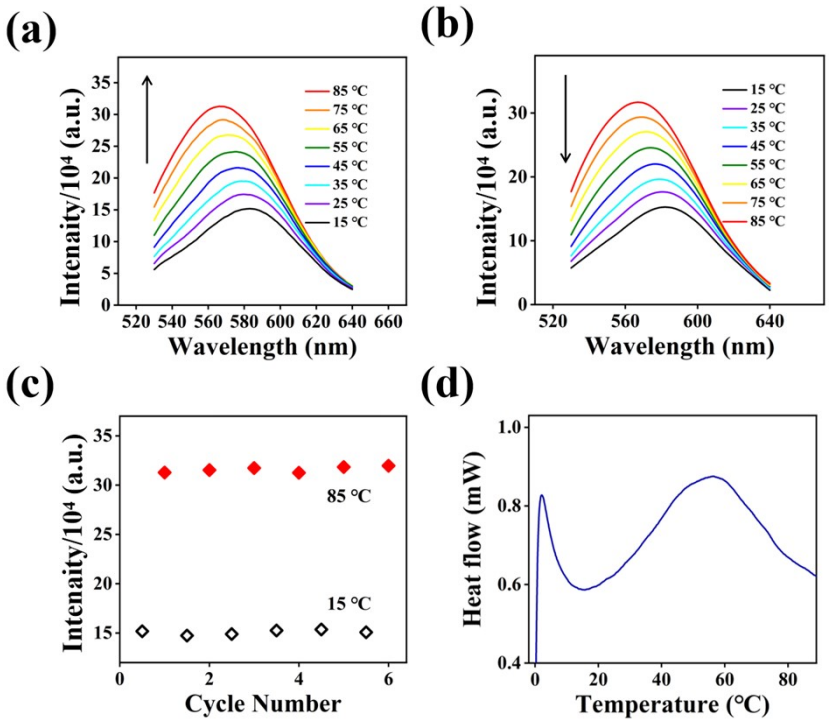

Figure S20 Fluorescence spectra of CDs-6 solution during heating (a) and cooling (b) processes. (c) Fluorescence spectra of CDs-6 solution at 15 °C and 85 °C during six cycles. (d) DSC curve of CDs-6.

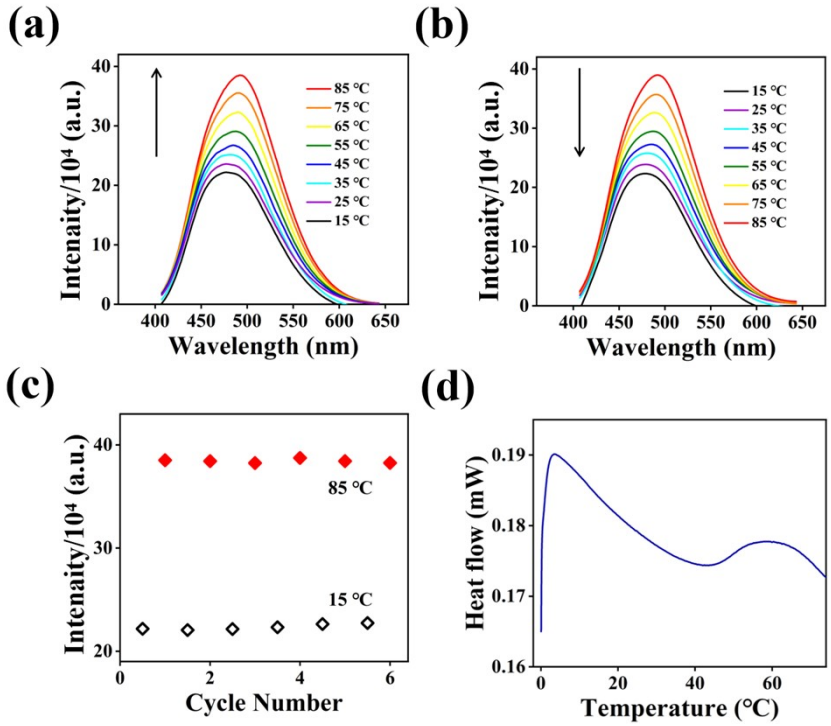

Figure S21 Fluorescence spectra of CDs-7 solution during heating (a) and cooling (b) processes. (c) Fluorescence spectra of CDs-7 solution at 15 °C and 85 °C during six cycles. (d) DSC curve of CDs-7.

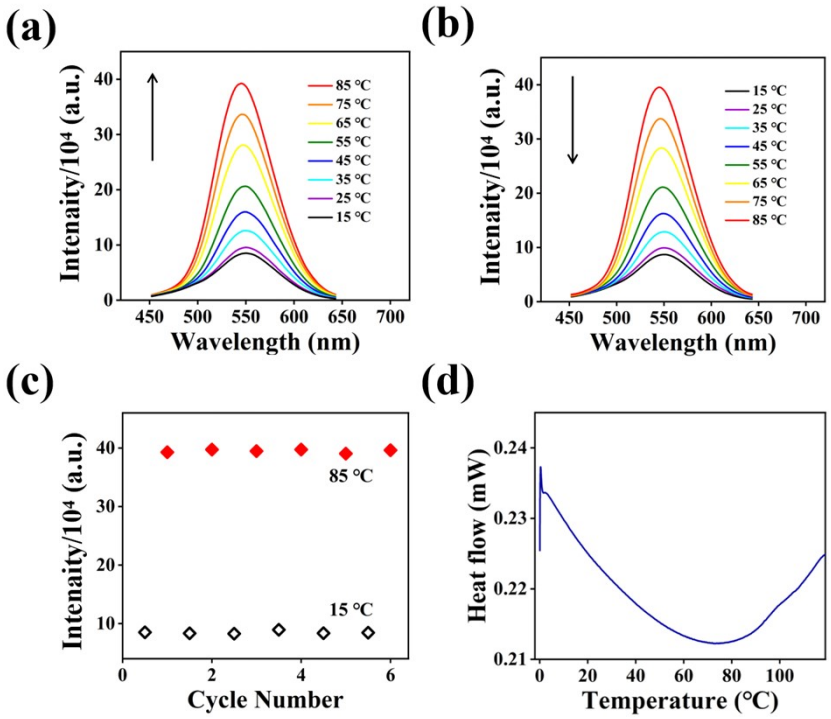

Figure S22 Fluorescence spectra of CDs-8 solution during heating (a) and cooling (b) processes. (c) Fluorescence spectra of CDs-8 solution at 15 °C and 85 °C during six cycles. (d) DSC curve of CDs-8.

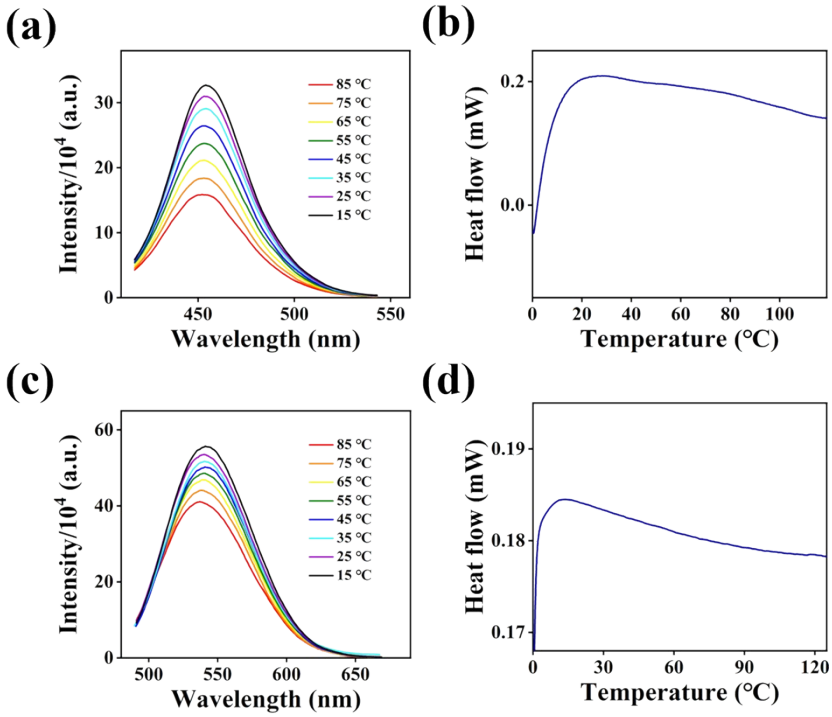

Figure S23 (a) Fluorescence spectra of blue-emitting CDs prepared from o-phenylenediamine and CA during the heating processes and (b) the corresponding DSC curve. (c) Fluorescence spectra of yellow-emitting CDs prepared from o-phenylenediamine and catechol during the heating

processes and (d) the corresponding DSC curve.

References

[1] Y. L. Xu, Y. Yang, S. Lin and L. H. Xiao, *Anal. Chem.,* 2020, **92**, 15632-15638.

[2] Q. Su, X. D. Wei, J. X. Mao and X. M. Yang, *Colloids Surf. A Physicochem. Eng. Aspects*, 2019, **562**, 86-92.

[3] C. Dong, M. S. Xu, J. H. Huang, F. Li, P. F. Wei, A. C. Tedesco and H. Bi, *ACS Appl. Nano Mater.,* 2020, **3**, 10560-10564.

[4] J.-R. Macairan, D. B. Jaunky, A. Piekny and R. Naccache, *Nanoscale Adv.*, 2019, **1**, 105-113.

[5] W. He, Z. X. Huo, X. Y. Sun and J. S. Shen, *Microchem. J.*, 2020, **153**, 104528.

[6] J. Zhang, D. Y. Nan, S. Pan, H. Liu, H. Yang and X. L. Hu, *Spectrochim. Acta. A Mol. Biomol. Spectrosc.,* 2019, **221**, 117161.

[7] Z. P. Zhu, Z. S. Sun, Z. Y. Guo, X. G. Zhang and Z. C. Wu, *J. Colloid Interface Sci.,* 2019, **552**, 572-582.

[8] C. X. Wang, Z. Z. Xu, H. Cheng, H. H. Lin, M. G. Humphrey and C. Zhang, *Carbon*, 2015, **82**, 87-95.

[9] X. B. Cui, Y. L. Wang, J. Liu, Q. Y. Yang, B. Zhang, Y. Gao, Y. Wang and G. Y. Lu, *Sens. Actuators B Chem.,* 2017, **242**, 1272-1280.

[10] C. Wang, T. T. Hu, T. J. Thomas, S. L. Song, Z. Q. Wen, C. X. Wang, Q. J. Song and M. H. Yang, *Nanoscale*, 2018, **10**, 21809-21817.

[11] Y. M. Yang, W. Q. Kong, H. Li, J. Liu, M. M. Yang, H. Huang, Y. Liu, Z. Y. Wang, Z. Q. Wang, T. K. Sham, J. Zhong, C. Wang, Z. Liu, S. T. Lee and Z. H. Kang, *ACS Appl. Mater. Interfaces,* 2015, **7**, 27324-27330.

[12] H. Zhang, J. J. You, J. H. Wang, X. Z. Dong, R. F. Guan and D. X. Cao, *Dyes Pigments,* 2020, **173**, 107950.

[13] J. H. Hua, Z. Mu, P. Hua, M. Wang and K. H. Qin, *Talanta*, 2020, **219**, 121279.

[14] W. D. Liu, S. M. Xu, Z. X. Li, R. Z. Liang, M. Wei, D. G. Evans and X. Duan, *Chem. Mater.,* 2016, **28**, 5426-5431.

[15] V. Nguyen, L. H. Yan, H. H. Xu and M. M. Yue, *Appl. Surf. Sci.,* 2018, **427**, 1118-1123.

[16] Z. X. Gan, Y. L. Hao and Y. Shan, *ChemNanoMat*, 2016, **2**, 171-175.